

## Domain growth kinetics and symmetry breaking in a thermally quenched system

This article has been downloaded from IOPscience. Please scroll down to see the full text article.

1992 J. Phys. A: Math. Gen. 25 6623

(<http://iopscience.iop.org/0305-4470/25/24/016>)

View [the table of contents for this issue](#), or go to the [journal homepage](#) for more

Download details:

IP Address: 171.66.16.59

The article was downloaded on 01/06/2010 at 17:45

Please note that [terms and conditions apply](#).

## Domain growth kinetics and symmetry breaking in a thermally quenched system

J Naudts†, J-F Willart‡ and M Descamps‡

† Departement Fysica, Universiteit Antwerpen, Universiteitsplein 1, B-2610 Antwerpen, Belgium

‡ Laboratoire de Dynamique des Cristaux Moléculaires, Université de Lille I, P5, 59655 Villeneuve d'Ascq Cédex, France

Received 6 May 1992, in final form 11 August 1992

**Abstract.** We simulate thermal quenches on a two-dimensional hard core model with symmetry breaking phase transition. By dividing large configurations into many small sub-squares lack of self-averaging is avoided and statistics are improved. Dynamic scaling is observed during more than two decades.

### 1. Introduction

The transformation kinetics of crystals thermally quenched below a phase transition temperature is an object of study of great importance in materials science. We are particularly interested in the specific case where:

(1) The system is quenched from a high-temperature disordered phase into a low-temperature ordered phase.

(2) The ordered phases are degenerate: the phase transition involves a spontaneous symmetry breaking.

(3) The order parameter is non-conserved: there are no conservation laws which can slow down the phase transformation kinetics.

The subject has been studied extensively in the literature (see e.g. [1] and the references quoted therein). In the case of a second-order transition the behaviour of the system can be summarized as follows. Immediately after the quench ordering sets in. On a larger time-scale the crystal is filled with ordered domains separated by anti-phase boundaries. The ordering proceeds by domain coarsening, i.e. by the motion of the boundaries.

If the final temperature is close to the critical temperature (i.e. a shallow quench) then the evolution of the local order parameter competes with the motion of domain boundaries on the same time scale. In this regime non-classical critical behaviour can be observed.

The current paper discusses a model which is well suited to study this kind of thermal quench. It is a hard-core model with a phase transition of the percolation type. No energy is gained by the formation of compact domains. As a consequence the domain growth is retarded. The evolution of the order parameter can be followed over many decades.

The next section discusses scaling relations. The model is introduced in section 3. Numerical simulation techniques are discussed in section 4. The results follow in section 5 and conclusions are given in section 6.

## 2. Scaling laws

Allen and Cahn [2] argued that the total surface  $S(t)$  of domain boundaries shrinks as  $1/\sqrt{t}$ , in agreement with experimental observation in binary alloys.  $S(t)$  is proportional to the residual energy  $\Delta E(t)$  which is the excess internal energy of the quenched phase compared to the ordered phase. The latter quantity is much easier to follow in numerical experiments. It seems to be generally accepted in literature (see e.g. [3–7]) that

$$\Delta E(t) \sim t^{-1/y} \quad (1)$$

with  $y = 2$ .

For quenches into the critical region slight deviations from  $y = 2$  should occur. In the theory of Allen and Cahn it is assumed that the order parameter has reached the equilibrium value. In the critical region local order is never reached because of critical slowing down [8]. Hence the basic assumption of ordered domains separated by domain walls is not satisfied.

The scaling theory of Milchev *et al* [1] predicts that in the critical region (1) should hold with

$$y = \frac{\nu z}{1 - \alpha} \quad (2)$$

where  $\alpha$  is the exponent of the specific heat:  $C_V \sim (T - T_c)^{-\alpha}$ ,  $\nu$  is the exponent of the correlation length:  $\xi \sim (T - T_c)^{-\nu}$  and  $z$  is the dynamical exponent [8]:  $\xi \sim t^{1/z}$ . The latter is given by (model A of [8])

$$z = 2 + c\eta \quad (3)$$

where  $\eta$  is the exponent of decay of the spatial correlation function  $g(r)$  at criticality:  $g(r) \sim r^{2-d-\eta}$ , and  $c$  is a numerical constant depending on the dimension  $d$ . Use of the mean field values  $\nu = 1/2$ ,  $\alpha = 0$ , and  $\eta = 0$ , gives  $z = 2$  and  $y = 1$ , in contradiction with the classical result  $y = 2$  (the Allen and Cahn prediction is not a mean field result).

The model studied in the current paper belongs to the universality class of the  $d = 2$  ferromagnetic Ising model with Glauber dynamics. On basis of numerical work and renormalization group results one expects a value of the dynamical exponent  $z$  close to 2 (most quoted values [9] are in the range  $2 \leq z \leq 2.2$ ; recently [17–19] a much larger value of  $z$  between (2.24) and (2.33) has been proposed). Combining the exact exponents  $\alpha = 0$  and  $\nu = 1$  with (2) gives  $y = z$ .

Sadiq and Binder [3] report results for a  $d = 2$  spin model with nearest and next to nearest neighbour interactions, belonging to a different universality class. They obtain a value  $y \simeq 2.1$  ( $1/y = 0.48$ ) at temperatures well below critical, and values varying between 2.5 and 3.0 for quenches into the critical region. These results have been confirmed in [10]. The estimated exponent values  $\nu \simeq 0.87$ ,  $\alpha \simeq 0.26$ , and  $z \simeq 2.4$ , yield  $y \simeq 2.85$  which should be valid in the critical region.

In view of these results one can expect that  $\gamma \simeq 2$  is generally valid for quenches with final temperature outside the critical region (but not too low in order to avoid freezing effects). In the critical region formula (2) should hold.

Also of interest is the time dependence of the order parameter  $M(t)$ . Shortly after the quench it has a small value because of the symmetry of the high temperature phase. Its average over many initial configurations  $\langle M(t) \rangle$  is exactly zero, and remains small until ordered domains grow to the size of the system. Hence the interesting quantity is the (time-dependent) static susceptibility  $\chi(t)$  which is the second moment of the distribution of  $M(t)$  (up to a constant factor)

$$k_B T \chi(t) = \frac{1}{N} \langle M^2(t) \rangle \tag{4}$$

( $N$  is the number of sites of the lattice; for simplicity of notation we assume a scalar order parameter).

The susceptibility and the residual energy should be related by [1]

$$\chi(t) \sim (\Delta E(t))^{-\gamma/(1-\alpha)} \tag{5}$$

where  $\gamma$  is the exponent of the static susceptibility  $\chi \sim (T - T_c)^{-\gamma}$  and  $\alpha$  is the exponent of the specific heat. The relation is explained as follows. During the quench the only thermodynamic parameter which evolves in time is the (internal) energy. One can associate an effective temperature  $T$  with the actual internal energy of the system. Then (5) states that the observed static susceptibility is nothing but the value corresponding to the effective temperature of the system.

### 3. The model

The model described below has been used in [11] to study domain growth kinetics in crystals where degenerate low-temperature phases repel each other strongly due to steric hindrance effects. The model is of interest because of its simplicity. It is well suited for the study of domain growth because it contains infinite repulsion terms which slow down the phase transformation kinetics.

At each site  $i$  of the square lattice a spin variable  $\sigma_i$  takes one of three possible values:  $\sigma_i = -1, 0$ , or  $1$ . Only two types of interactions are present:

(a) A chemical potential  $\mu$  favours the  $\sigma = \pm 1$  states.

(b) An infinite repulsion forbids  $\sigma_i = 1$  and  $\sigma_j = -1$  on neighbouring sites ( $|i - j| = 1$ ).

The same model but with an additional attraction between non-zero equal spins on neighbouring sites has been studied in [7]. A slightly modified model is exactly solvable [15] on the triangular lattice.

The model can be seen as a special case of the Blume–Emery–Griffiths (BEG) model Hamiltonian [12–14]

$$H = -J \sum_{(i,j)} \sigma_i \sigma_j - K \sum_{(i,j)} \sigma_i^2 \sigma_j^2 + D \sum_i \sigma_i^2 \tag{6}$$

with  $J \rightarrow +\infty$ ,  $K = -J$ , and  $D = -\mu$ . The existence of a phase transition in the present model has been proved in [20] (see also [21]). The  $K = -J$  case of the

BEG model has been studied in [14]. From the latter work one can conclude that the present model has a second order phase transition as a function of temperature.

The relevant parameter of the model is the activity  $\lambda = \exp(-\mu/k_B T)$ . At high activity the  $\sigma = +1$  and  $-1$  values have the same occurrence on average. Below the critical value  $\lambda_c \simeq 0.55$  symmetry breaking occurs with order parameter  $\langle \sigma \rangle \neq 0$  (see the appendix).

#### 4. Numerical techniques

Let  $N$  denote the number of sites. During one elementary Monte Carlo step (MCS)  $N$  sites are selected and changed according to the following prescription:

- (1) A site  $i$  and a new spin value  $\sigma$  ( $= 0, 1, \text{ or } -1$ ) are selected at random.
- (2) If the selected spin  $\sigma_i$  and the new value  $\sigma$  are either both zero or both non-zero then no change takes place.
- (3) If the selected spin  $\sigma_i$  is non-zero and the new value  $\sigma$  is zero then  $\sigma_i$  is set to zero with probability  $\lambda$ .
- (4) If the selected spin  $\sigma_i$  is zero and the new spin value  $\sigma$  is non-zero then  $\sigma_i$  obtains the value  $\sigma$  except when this would lead to opposite values  $+1$  and  $-1$  on neighbouring sites.

The simulations can be speeded up by use of the following algorithm:

- (1) A site  $i$  is selected at random.
- (2) If  $\sigma_i \neq 0$  then  $\sigma_i$  is cleared to zero with probability  $\lambda/2$ .
- (3) If  $\sigma_i = 0$  then a new value  $\sigma = \pm 1$  is chosen at random, and  $\sigma_i$  is put equal to  $\sigma$ , except when this would lead to a conflict with the spin value on neighbouring sites.

It is easy to see that three updates by the former algorithm are equivalent with two updates by the latter. The times mentioned in the current paper refer to the faster of the two algorithms.

During the simulations we monitor the density  $\rho(t) = N^{-1} \sum_i \sigma_i^2$  of non-zero spins ( $N$  is the number of sites of the configuration) and the probability distribution  $P_L(M(t))$  of the total magnetization  $M(t) = \sum_i \sigma_i$  of configurations of size  $L \times L$ . The residual energy  $\Delta E(t)$  is related to the density  $\rho(t)$  by

$$\Delta E(t) = \mu N(\rho(\infty) - \rho(t)). \quad (7)$$

The probability distribution  $P_L(M(t))$  has been established by measuring the total magnetization  $M$  of all sub-squares of sizes  $32 \times 32$ ,  $64 \times 64$  and  $128 \times 128$  within large systems consisting of  $1024 \times 1024$  lattice sites (using periodic boundary conditions on the large system). We can expect that in this way the boundary effects are heavily reduced while at the same time very good statistics result from the large number of small sub-squares. Our data shows that at least  $L$  sub-squares of size  $L \times L$  are needed to obtain acceptable results, hence we limit ourselves to sub-squares of size  $L \leq 128$ . A similar increase of fluctuations with increasing size of the configuration has been reported in [3]. It has been called [1] 'lack of self-averaging'. From  $P_L(M(t))$  we calculate the average magnetization  $m_L(t)$  and the static susceptibility  $\chi_L(t)$ .

#### 5. Simulation results

The simulations reported here are done for  $\lambda = 0.50$ . The initial configuration has all spin variables  $\sigma_i$  equal to zero.

The time-dependent density  $\rho(t)$  is shown in figure 1. A fit with

$$\rho(t) = \rho(\infty) - At^{-1/y} \quad (8)$$

(which follows from (1) and (7)) from  $t = 32$  to 1024 MCS (8 to 16 independent simulations) gives  $\rho(\infty) = 0.603(2)$  and  $y = 2.08(+0.22, -0.16)$ . The relative RMS error of the three-parameter fit is  $3 \times 10^{-4}$ . Note that there are important differences between different runs, mainly resulting in a large error (20%) on the amplitude  $A$ .

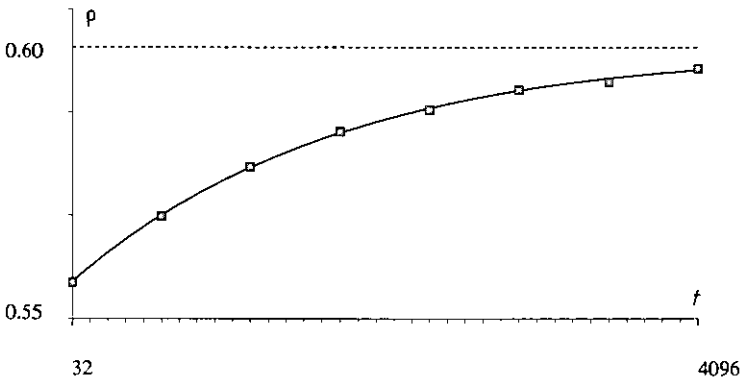


Figure 1. Density of non-zero spins as a function of time (logarithmic scale); the line is the fitted curve discussed in the text.

The time dependence of  $\chi_L$  averaged over many small configurations is shown in figure 2. On a short time scale it increases linearly as expected: starting from an initially homogeneous configuration the  $\sigma = 0$  sites are changed randomly into  $\sigma = \pm 1$  sites. Hence the total magnetization  $M$  performs a one-dimensional random walk. In particular the formula

$$k_B T \chi(t) = 2t \quad (9)$$

should hold on a short time scale. For  $t \ll 1$  MCS relation (9) is indeed found to be satisfied within numerical accuracy. At intermediate times the increase of  $\chi$  slows down. The average slope is about 0.8 instead of 1. In this regime the spontaneous ordering of the system is hindered by the competition of two types of ordered domains.

In order to clarify the finite size effects, two types of simulation results are compared in figure 2: (i) simulations on small systems with periodic boundary conditions, and (ii) averages over many sub-squares of large configurations of  $1024 \times 1024$  sites. It is clear from figure 2 that finite size does effect the simulations for times  $t > 16$  in the  $32 \times 32$ -case and  $t > 256$  in the  $64 \times 64$  case. We can understand the finite size effect as being due to amplification of the ordering mechanism. Indeed, when a small system orders, then, by the periodic boundary conditions it sees the neighbouring copies of itself order as well. The influence of the latter will amplify the ordering process. On the other hand, an ordering sub-square of a large configuration sees neighbouring sub-systems which maybe do not order or have an average order parameter of the opposite sign. Hence the ordering of the sub-square is slowed down.

In this way one can understand that periodic boundary conditions on a small system can amplify the ordering process.

When comparing different simulation runs, it appears that there is a strong correlation between the average value of the susceptibility  $\chi_L(t)$  and the actual value of the density  $\rho(t)$ . For that reason we have studied  $\chi_L$  as a function of  $\rho$ .

The data of  $\chi_L(t)$  for  $L = 32$ , averaged over 1024 sub-squares and 8 to 16 runs, and the data of  $\rho(t)$ , with  $t$  varying from 32 to 1024 MCS, have been fitted using the formula

$$A(\rho(\infty) - \rho(t))^{-\gamma/(1-\alpha)} \quad (10)$$

(derived from (5) using (7)). The result of this three-parameter fit is  $\rho(\infty) = 0.612(+0.008, -0.005)$  and  $\gamma/(1-\alpha) = 1.76(+0.44, -0.29)$ . The relative RMS error of the fit is  $4 \times 10^{-3}$ . The value obtained for  $\rho(\infty)$  deviates slightly from the one quoted at the start of the section.

The data for  $\chi_L(t)$  with  $L = 64$  or 128 could not be analysed properly. The statistics deteriorate because data from fewer sub-squares is available. On the other hand, the sampling problem is much worse due to the larger configuration space.

Initially the probability distribution  $P_L(M(t))$  is Gaussian. As a function of time the width of the distribution increases and deviates from the Gaussian shape in the vicinity of  $M = 0$ . The shape becomes nearly rectangular at  $t = 4196$  MCS. This peculiar time dependence of  $P_L(M(t))$  can best be understood in terms of a time-dependent Ginzburg–Landau free energy  $F_t(M)$  defined by

$$F_t(M) = -k_B T \log P_L(M(t)) \quad (11)$$

Initially,  $F_t(M)$  is a narrow parabola whose width increases with time. At the end the potential is completely flat near the origin. See figure 3.

## 6. Conclusions

By numerical simulation of thermal quenches we have verified that two predictions of the scaling theory of [1], i.e. formulae (1) and (5), hold to great accuracy in a simple  $d = 2$  spin lattice model. In this way two critical exponents could be determined. Relation (5) holds with  $\gamma/(1-\alpha) \simeq 1.76$ , close to the value  $7/4$  expected for the  $d = 2$  Ising model. Relation (1) holds with  $y \simeq 2.08$ , close to the value  $y = 2$  predicted by the classical theory of Allen and Cahn. It implies a dynamic exponent  $z = 2.08$ , in agreement with values reported in the literature (e.g. [16]  $z = 2.076(5)$ ).

The results obtained for the static susceptibility  $\chi(t)$  and for the probability distribution of the total magnetization  $M(t)$  indicate that as a function of time the system evolves towards criticality. On small systems deviations from scaling behaviour set in rather early because of an amplification effect induced by periodic boundary conditions. By considering  $L \times L$  sub-squares of large configurations we could avoid such effects due to the boundary conditions. Then the scaling behaviour is observable over more than two decades.

From the probability distribution of the total magnetization  $M(t)$  a Ginzburg–Landau free energy can be calculated. At later times it is a wide potential, nearly flat at the origin. There is no evidence for potential minima around non-zero values  $\pm M_0$  of the order parameter. This is only expected to be the case at much later times. Even at  $t = 4096$  MCS, local order is not established on the length scale of 32 lattice sites.

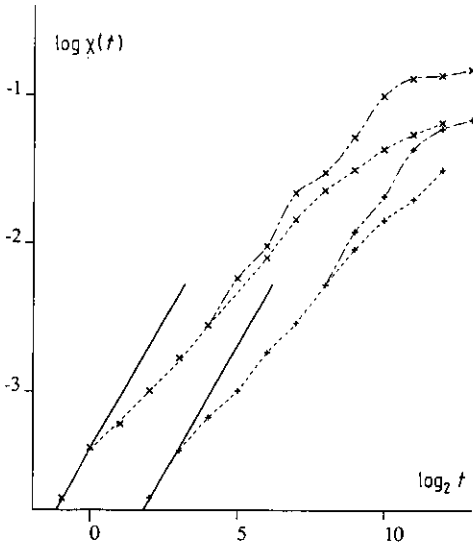


**Figure 2.** Static susceptibility as a function of time. The average is taken over 80 independent simulations of a  $32 \times 32$  system ( $x$ ) and over 100 independent simulations of a  $64 \times 64$  system ( $+$ ), resp. Also shown are the averages over square sub-sets of configurations with size  $1024 \times 1024$  (16 independent simulations for  $t \leq 256$ , 8 independent simulations for  $t = 512, 1024$ , 1 simulation for  $t = 2048, 4096$  — lower curves). The full lines are the theoretical prediction valid at early times. The dashed curves are guides for the eye. The results for the different sizes are shifted vertically in order to avoid overlap.

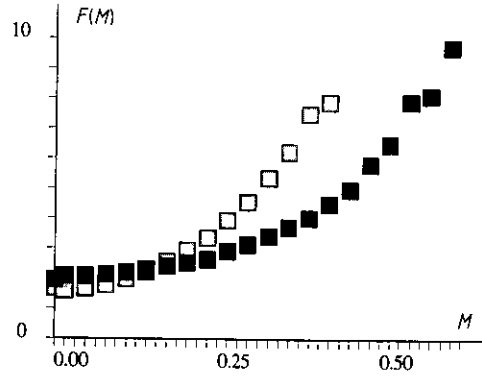


**Figure 3.** Free energy as a function of magnetization for  $32 \times 32$  sub-squares of a  $1024 \times 1024$  configuration (16 independent simulations) at times  $t = 64$  (light) and  $t = 256$  MCS (dark).

### Acknowledgments

This work is supported by EEC Science contract SC1-0426-C(CD). We thank Professor J L Lebowitz for drawing our attention to [20, 21].

### Appendix

In order to estimate the value of  $\lambda_c$  we studied the correlation length  $\xi$  as a function of temperature  $T$ . The configurations were initialized either in the ground state  $\sigma_i = 1$  or in the high temperature state  $\sigma_i = 0$ . The correlation length was measured after a fixed simulation time ( $t = 1000$  MCS).

In the high temperature phase  $T > T_c$  the system relaxes exponentially with time and the results of simulations with both types of initial conditions coincide within numerical precision. At low temperatures  $T < T_c$  the simulations starting from the ground state configuration show rapid relaxation while, due to the symmetry breaking problem, the simulations starting from the  $\sigma = 0$  state do not relax to the equilibrium phase on the time scale of the numerical experiment. As a consequence, both types



of simulation yield results which disagree with each other. The correlation length is particularly sensitive to discriminating the equilibrium and non-equilibrium phases. See figure A1.

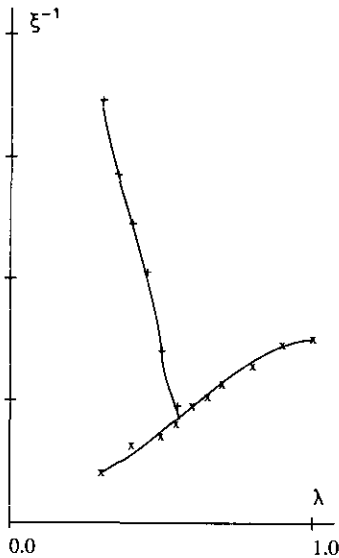


**Figure A1.** Inverse correlation length  $1/\xi$  as a function of  $\lambda$  with initial configuration  $\sigma_i = 0$  (x) and  $\sigma_i = 1$  (+), in arbitrary units.

Measuring at a later time  $t$ , i.e. after a longer relaxation time, results in a further increase of the correlation length in the metastable low temperature phase.

## References

- [1] Milchev A, Binder K and Heermann D W 1986 *Z. Phys.* B **63** 521
- [2] Allen S M and Cahn J W 1979 *Acta Metall.* **27** 1085
- [3] Sadiq A and Binder K 1984 *J. Stat. Phys.* **35** 517
- [4] Kumar S, Viñals J and Gunton J D 1986 *Phys. Rev. B* **34** 1908
- [5] Roland C and Grant M 1989 *Phys. Rev. Lett.* **63** 551
- [6] Gawliński E T, Grant M, Gunton J D and Kaski K 1985 *Phys. Rev. B* **31** 281
- [7] Willart J F, Mouritsen O G, Naudts J and Descamps M 1992 *Phys. Rev. B* in press
- [8] Hohenberg P C and Halperin B I 1977 *Rev. Mod. Phys.* **49** 435
- [9] Lage E J S 1987 *Physica* **140A** 629 table 1 and references
- [10] Høst-Madsen A, Shah P J, Hansen T V and Mouritsen O G 1987 *Phys. Rev. B* **36** 2333
- [11] Willart J F, Naudts J and Descamps M 1990 *Phase Transitions* **31** 261
- [12] Blume M, Emery V J and Griffiths R B 1971 *Phys. Rev. A* **4** 1071
- [13] Berker A N and Wortis M 1976 *Phys. Rev. B* **14** 4946
- [14] Wang Y Li, Lee F and Kimel J D 1987 *Phys. Rev. B* **36** 8945
- [15] Nienhuis B 1991 *Physica* **177A** 109
- [16] Mori M and Tsuda Y 1988 *Phys. Rev. B* **37** 5444
- [17] Rogiers J and Indekeu J O 1990 *Phys. Rev. B* **41** 6998
- [18] Poole P and Jan N 1990 *J. Phys. A: Math. Gen.* **23** L453
- [19] MacIsaac K and Jan N 1992 *J. Phys. A: Math. Gen.* **25** 2139
- [20] Lebowitz J L and Gallavotti G 1971 *J. Math. Phys.* **12** 1129
- [21] Runnels L K and Lebowitz J L 1974 *J. Math. Phys.* **15** 1712